Quantum electrodynamical torques in the presence of Brownian motion

New Journal of Physics
The open-access journal for physics

Quantum electrodynamical torques in the presence of Brownian motion

Jeremy N Munday[1], **Davide Iannuzzi**[2] **and Federico Capasso**[3,4]

[1] Department of Physics, Harvard University, Cambridge, MA 02138, USA
[2] Department of Physics and Astronomy, Faculty of Sciences, Vrije Universiteit, Amsterdam, 1081HV, The Netherlands
[3] Division of Engineering and Applied Sciences, Harvard University, Cambridge, MA 02138, USA
E-mail: capasso@deas.harvard.edu

New Journal of Physics **8** (2006) 244
Received 23 June 2006
Published 20 October 2006
Online at http://www.njp.org/
doi:10.1088/1367-2630/8/10/244

Abstract. Quantum fluctuations of the electromagnetic field give rise to a zero-point energy that persists even in the absence of electromagnetic sources. One striking consequence of the zero-point energy is manifested in the Casimir force, which causes two electrically neutral metallic plates to attract in order to reduce the zero-point energy. A second, less well-known, effect is a torque that arises between two birefringent materials with in-plane optical anisotropy as a result of the zero-point energy. In this paper, we discuss the influence of Brownian motion on two birefringent plates undergoing quantum electrodynamical (QED) rotation as a result of the system's zero-point energy. Direct calculations for the torque are presented, and preliminary experiments are discussed.

[4] Author to whom any correspondence should be addressed.

PII: S1367-2630(06)27240-9

Contents

1. Introduction

Even in the absence of electromagnetic sources, there exist quantum fluctuations of the electromagnetic field that lead to a nonzero energy density, i.e. the zero-point energy, which exists both in vacuum and in dielectric media. In 1948, Casimir predicted the existence of an attractive force between two grounded metallic plates in vacuum as a result of this zero-point energy density [1]. Confinement of these fluctuations by the boundary conditions at the plates causes a modification of the zero-point energy that varies with distance and leads to this attractive force. Lifshitz then generalized this theory to calculate the force between two isotropic materials of arbitrary dielectric function immersed in a third medium also of arbitrary dielectric function [2]. For small separations, the result provides a complete description of the van der Waals interaction [3, 4]. For larger separations, when the two outer materials are taken to be ideal metals and the intervening material is taken to be vacuum, Lifshitz's result reduces to that of Casimir. Experiments have since been performed and are in excellent agreement with this theory [5]–[12] (see, however, comments on claimed precision in some experiments [13]–[17]).

The effect of the zero-point energy between two optically anisotropic materials, as shown in figure 1, has also been considered [18]–[24]. In this case, the fluctuating electromagnetic fields have boundary conditions that depend on the relative orientation of the optical axes of the materials; hence, the zero-point energy arising from these fields also has an angular dependence. This leads to a torque that tends to align two of the principal axes of the materials in order to minimize the system's energy. We have recently shown that such torques should indeed be measurable and have suggested an experimental configuration to perform these measurements [20].

In this paper, we consider some of the problematic features of this latter experiment and suggest a modified experimental approach involving Brownian motion that should solve these problems.

2. Theory of the quantum electrodynamical (QED) torque

In 1972, Parsegian and Weiss derived an expression for the short range, non-retarded van der Waals interaction energy between two semi-infinite dielectrically anisotropic materials immersed

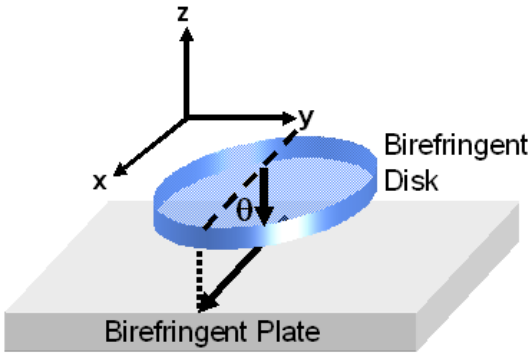

Figure 1. Schematic of the system under investigation. Two birefringent plates with in-plane optical anisotropy are placed at close proximity with angle θ between their optical axes.

within a third material [18]. This result, obtained by the summation of the electromagnetic surface mode fluctuations, showed that the interaction energy was inversely proportional to the separation squared and depended on the angle between the optical axes of the two anisotropic materials. In 1978, Barash independently derived an expression for the interaction energy between two anisotropic materials using the Helmholtz free energy of the electromagnetic modes, which included retardation effects [19]. In the non-retarded limit, Barash's expression confirmed the inverse square distance dependence of Parsegian and Weiss and that the torque, in this limit, varies as $\sin(2\theta)$, where θ is the angle between the optical axes of the materials.

The equations that govern the torque are quite cumbersome and are treated in detail elsewhere [19, 20]. For brevity, we refer the reader to those papers for a more in-depth analysis and simply state a few of the relevant results. Firstly, the torque is proportional to the surface area of the interacting materials and decreases monotonically with increasing surface separation. Secondly, to a good approximation, it is found that the QED torque at a given distance varies as:

$$M \cong A \sin(2\theta), \tag{1}$$

even in the retarded limit, where A is the value of the torque at $\theta = \pi/4$. Figure 2(a) shows the torque as a function of angle for a 2 μm diameter lithium niobate disk suspended in water above a calcite plate at a distance of $d = 50$ nm. The details of this configuration will be described shortly. The $\circ$ correspond to values of the torque calculated according to the procedure of [20], while the solid line corresponds to a best fit of (1). It can easily be seen that (1) is indeed an excellent fit to the calculated points.

Because the torque is obtained as an angular derivative of the potential energy, i.e $M = -\mathrm{d}U(\theta)/\mathrm{d}\theta$, we can approximate the energy associated with this angular dependence as:

$$U(\theta) = -\int M \mathrm{d}\theta \cong \tfrac{1}{2} A \cos(2\theta). \tag{2}$$

Figure 2(b) shows the angular dependence of the energy. Note that the minimum energy occurs at zero and π, corresponding to the alignment of the optical axes, while the maximum energy occurs at $\pi/2$, corresponding to the alignment of the optical axis of the disk with a second

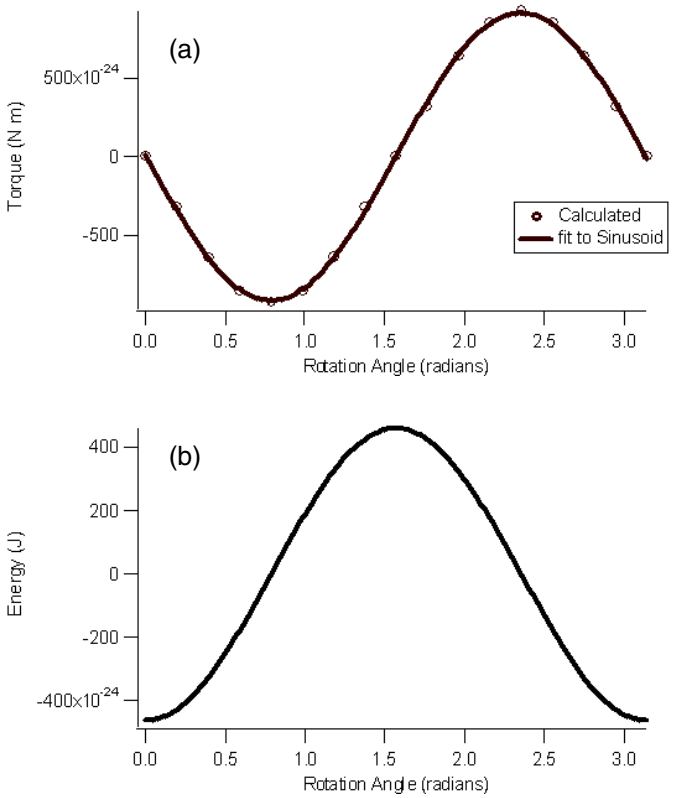

Figure 2. Calculations of the QED torque and energy between a $LiNbO_3$ disk and a calcite plate. (a) Calculated torque (○) and sinusoidal fit (line). (b) Calculated energy from sine fit of panel (a).

principal axis of the plate. Also from the figure, it is apparent that there are stable equilibria at zero and π, where the deviations from these angles result in torques rotating the disk back to zero and π, respectively, and an unstable equilibrium at $\pi/2$, where angular deviations from $\pi/2$ result in a torque driving the disk away from $\pi/2$.

It is now important to ask whether such an effect could be observable. Because the torque is proportional to the area of interaction and increases for decreasing separations, we would like to use large disks in close proximity. It may first be tempting to consider a torsional setup where one disk is suspended from a thin rod above a birefringent plate in vacuum and is allowed to rotate under the influence of this QED torque. However, at such short distances ($\leqslant$100 nm), it is very difficult to keep two large surfaces (tens of microns) parallel, due to the attractive Casimir–Lifshiftz force, and free of dust and other contaminants. If one could instead use a repulsive force to balance a disk above a plate, this problem could be eliminated. We recently suggested such an experiment, which should be capable of observing this phenomenon between barium titanate ($BaTiO_3$) and calcite or quartz in ethanol [20]. The main idea is as follows: the Casimir–Lifshitz force is always attractive between two identical materials; however, the force can become repulsive when two different materials are submerged in a third medium if their dielectric functions, evaluated at imaginary frequency, obey the following relationship [3, 4]:

$$\varepsilon_{\text{Plate}}(i\omega) < \varepsilon_{\text{Fluid}}(i\omega) < \varepsilon_{\text{Disk}}(i\omega) \quad \text{or} \quad \varepsilon_{\text{Plate}}(i\omega) > \varepsilon_{\text{Fluid}}(i\omega) > \varepsilon_{\text{Disk}}(i\omega). \qquad (3)$$

Two material combinations that satisfy this criterion are $BaTiO_3$–ethanol–calcite and $BaTiO_3$–ethanol–quartz. These combinations will give rise to a repulsive Casimir–Lifshiftz force which will counterbalance the weight of the disk and allow it to float at a predetermined distance above the plate. For a 20 μm thick calcite disk with a 40 μm diameter above a $BaTiO_3$ plate in ethanol, the equilibrium separation was calculated to be approximately 100 nm with a maximum torque of approx. 4×10^{-19} Nm [20]. For observation of this torque, it was suggested that the disk be rotated to $\theta = \pi/4$ between the optical axes of the two birefringent materials by means of the transfer of angular momentum of light from a polarized beam. The laser could then be shuttered, and one would visually observe the rotation of the disk back to its minimum energy orientation. This motion is described by [20]

$$I_{\text{rot}}\ddot{\theta} = A\sin(2\theta) - \frac{\pi\eta R^4}{2d}\dot{\theta}, \tag{4}$$

where $I_{\text{rot}} = \frac{1}{2}mR^2$ is the moment of inertia of a disk of radius R and mass m, η is the viscosity of the fluid, d is the separation between the disk and the plate, and $A\sin(2\theta)$ is the QED torque from (1). For a calcite disk initially at $\theta = \pi/4$, QED rotation of a few degrees should be observable on the timescale of 10 min.

Experimentally, this scheme has proven somewhat difficult. Firstly, it relies on a long-range QED repulsion which has not been accurately measured, in general, or even shown to exist for these particular materials[5]. This makes it hard to determine the direct cause of floatation or the distance between the disk and the plate. Secondly, disks can easily encounter contaminants when the timescale is tens of minutes, which causes the disks to stop floating. Thirdly, alignment of laser optics in real time as the disk moves provides a further complication. While these issues are not insurmountable, it is worth asking whether there is an alternative measurement and detection scheme that could also be pursued. In the next section, we will describe an alternative set-up that alleviates many of the previously mentioned difficulties and should lead to a direct measurement of the orientation dependence of the QED energy.

3. A statistical approach and influence of Brownian motion

As stated previously, the driving QED torque is proportional to the surface area of the disk; however, the damping torque due to the viscosity of the fluid between the disk and the plate, given by the last term in (4), goes as R^4. Thus, in order to reduce the time evolution of the disk to shorter timescales, the surface area of the disks should be reduced. However, because this reduces the torque as well, the energy scale of the torque will become comparable to or less than the thermal energy, $k_{\text{B}}T \cong 4.14 \times 10^{-21}$ J. Brownian motion will therefore become increasingly important as the diameter of the disk decreases. The timescale of the Brownian rotation is set by the rotational diffusion coefficient. For a thin disk of radius $R = 1$ μm far away from any surfaces, the rotation diffusion coefficient is $D_{\text{r}} \cong 3k_{\text{B}}T/32\eta R^3 \approx 0.39\,\text{rad}\,\text{s}^{-1}$ [26] for $\eta = 1.0 \times 10^{-3}\,\text{N}\,\text{s}\,\text{m}^{-2}$. For a disk near a wall this value will be further reduced; however, by modifying the radius, different regimes can be explored.

When Brownian rotations become comparable to the QED rotation, the disk will no longer rotate smoothly to its minimum energy configuration. Instead the angle between the optical axes

[5] A few less precise measurements of repulsive close range (approx a few nanometres) van der Waals forces have been reported in [25].

will fluctuate to sample all angles. The probability distribution for the observation of the angle θ between the two optical axes is:

$$p(\theta) = \alpha \exp\left[-U(\theta)/k_{\mathrm{B}}T\right], \tag{5}$$

where $U(\theta)$ is the potential energy of the QED orientation interaction, i.e. the energy associated with the torque, and α is a normalization constant such that $\int p(\theta)\,\mathrm{d}\theta = 1$. By observing the angle between the axes as a function of time, one can deduce the probability distribution via a histogram of the angular orientations. This is similar to the way in which potential energy as a function of distance is determined in total internal reflection microscopy (TIRM) experiments [27, 28].

In the next section we describe an experimental apparatus to observe this phenomenon.

4. Experimental configuration

To observe this effect, we need to levitate a birefringent disk above a birefringent plate at short range and be able to detect the orientation of the axes. We will address both of these issues in order in the next two subsections. Finally, we will describe the experimental configuration being used to detect the QED toque and show initial measurements with non-birefringent particles.

4.1. Levitation scheme

In the previously described experimental configuration [20], a repulsive Casimir–Lifshitz force was the mechanism for levitation; however, as mentioned, such an interaction has not been carefully studied through experiment, and it is worthwhile to consider alternative methods. A more well-characterized and adjustable levitation scheme is that of the double layer repulsion [4]. By adding a surfactant (e.g. sodium dodecylsulfate, which is commonly known as SDS) to an aqueous solution containing particles or disks, an electrostatic repulsion is achieved as the hydrophobic ends of the surfactant molecules attach to the interacting surfaces. This causes charge buildup on both surfaces (plate and disk) of the same sign and leads to a repulsion, which is often used in colloidal suspensions [4, 29]. By adding an electrolyte (e.g. NaCl), we can adjust the Debye screening length of the charged surfaces and hence modify the equilibrium separation between the disk and the plate. The equilibrium separation occurs when the sum of the forces (Casimir–Lifshitz, double layer and weight) acting on the particle is zero:

$$\sum F = F_{\mathrm{CL}}(d) + D \times \exp\left[-d/l\right] - \pi R^2 h \Delta\rho g = 0, \tag{6}$$

where $F_{\mathrm{CL}}(d)$ is the Casimir–Lifshitz force at distance d, D is a constant related to the Poisson–Boltzmann potential evaluated at the surface due to charging, l is the Debye length, R is the radius of the disk, h is the thickness of the disk, $\Delta\rho$ is the density difference between the disk and the solution, and g is the acceleration due to gravity. Both the Casimir–Lifshitz force and the weight of the disks are set by the geometry of the system and the materials chosen; however, the double layer force can be modified by changing the electrolytic concentration. Thus, the floatation height can be adjusted in this way. For the remainder of this discussion, we will focus on a setup which consists of a circular $LiNbO_3$ disk with $R = 1\ \mu$m and $h = 0.5\ \mu$m in an aqueous solution with SDS and NaCl chosen for a levitation height of 50 nm above a calcite plate. Figure 3 shows the

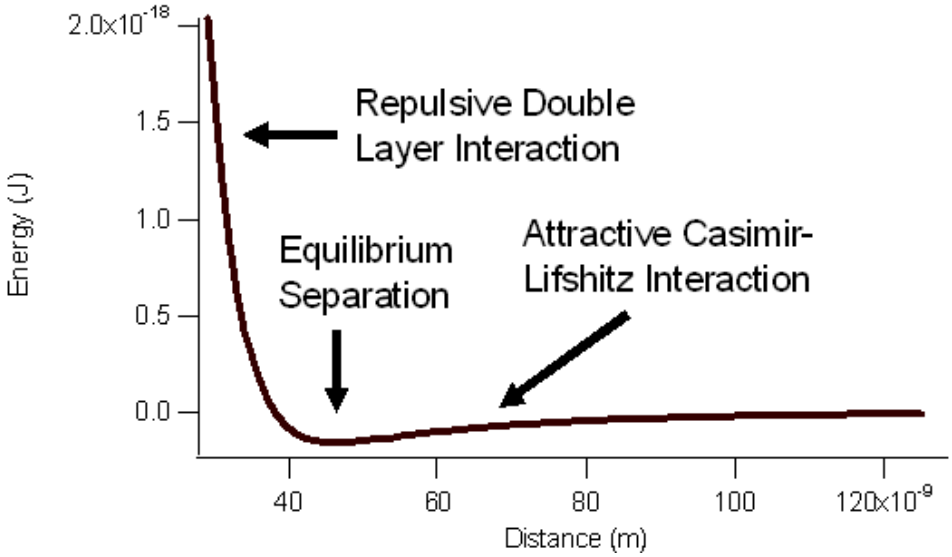

Figure 3. Energy as a function of separation between a $LiNbO_3$ disk and a calcite plate including contributions from the double layer interaction (dominant at close range), the Casimir–Lifshitz interaction (dominant at longer range) and gravity (negligible). Equilibrium is obtained around 50 nm.

approximate interaction energy following from the forces of (6), where we have assumed that the double layer interaction can roughly be modelled using the *weak overlap approximation* [4] with similar surface potentials of 100 mV on each surface and an NaCl concentration of 5 mM. Further, the Casimir–Lifshitz interaction was modelled using a composite dielectric function for each birefringent material by averaging the dielectric functions of the three principal axes. The equilibrium separation is found to be 46 nm with deviations of a few nanometres due to thermal energy of the order $k_B T$.

4.2. Determination of the angular orientation θ

In order to track the motion of the disk above the plate, we use a video microscopy set-up similar to the one described in [30]. The disk's motion is tracked and recorded as is the intensity of the transmitted light. The orientation of the disk is determined by placing it between crossed polarizers (or a similar combination of optical components), so that the intensity of the transmitted light can be related to the orientation of the optical axis. In order to determine the expected optical intensity at the output as a function of θ , we use the Jones matrix representation of the optical elements to determine the exiting E-field from which the intensity is calculated [31, 32]. For a polarized beam travelling in the z-direction which goes through a single optical element, the exiting E-field is given by:

$$E_{\text{out}} = ME_{\text{in}} = \begin{bmatrix} m_{11} & m_{12} \\ m_{21} & m_{22} \end{bmatrix} \begin{bmatrix} E_x \\ E_y \end{bmatrix}, \tag{7}$$

where the values of m_{ij} depend on the chosen optical component. The simplest setup one might think to use could consist of a birefringent disk free to rotate above a birefringent plate, which is

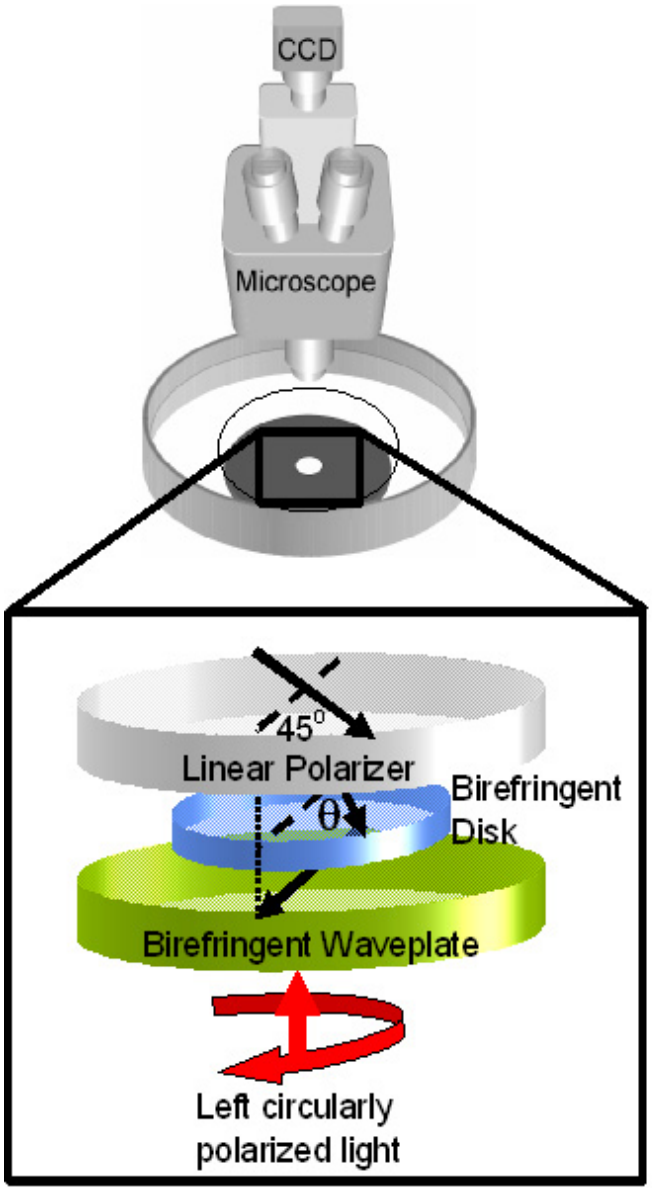

Figure 4. A sketch of the experimental setup used to determine the angular dependence of the zero-point energy between birefringent plates.

placed between crossed polarizers. By putting the two birefringent materials between the crossed polarizers, the intensity of transmitted light will depend on the angular orientation of the two materials. However, a detailed calculation of the intensity profile as a function of θ, shows that the intensities corresponding to the minimum and maximum energy configurations of the plate and disk are the same, i.e. the orientation cannot be determined by the intensity measurement alone. To solve this problem, we use the following configuration, as shown in figure 4: left hand circularly polarized light incident on a birefringent half-wave plate and suspended disk, which is free to rotate, followed by a linear polarizer with transmission axis at 45° with respect to the

optical axis of the birefringent plate. The output field is then given by:

$$E_{\text{out}} = \underbrace{M_{\text{linear45}}}_{\text{final polarizer}} \Bigg[\underbrace{\overbrace{R(\theta)}^{\text{rotation matrix}} \quad M_{\text{Disk}} \quad \overbrace{R(-\theta)}^{\text{rotation matrix}}}_{\text{disk at arbitrary}} \Bigg] \underbrace{M_{\text{HWP}}}_{\text{birefringent plate}} \overbrace{E_{\text{in}}}^{\substack{\text{indent left circularly} \\ \text{polarixed light}}} , \tag{8}$$

where

$$M_{\text{linear45}} = \frac{1}{2}\begin{bmatrix} 1 & 1 \\ 1 & 1 \end{bmatrix}, \quad R(\theta) = \begin{bmatrix} \cos(\theta) & -\sin(\theta) \\ \sin(\theta) & \cos(\theta) \end{bmatrix},$$

$$M_{\text{Disk}} = \begin{bmatrix} e^{-i\phi/2} & 0 \\ 0 & e^{i\phi/2} \end{bmatrix}, \quad M_{\text{HWP}} = \begin{bmatrix} -i & 0 \\ 0 & i \end{bmatrix}, \quad E_{\text{in}} = \frac{1}{\sqrt{2}}\begin{bmatrix} 1 \\ i \end{bmatrix}.$$

The intensity is proportional to the sum of the squared **E**-field components and is given by:

$$I \propto \tfrac{1}{2}[1 - \cos(2\theta)]\sin(\phi)\,, \tag{9}$$

where $\phi = 2\pi h\,\Delta n/\lambda$ is the phase retardation due to the birefringent disk of thickness h with a difference in indices between principal axes of Δn for light of wavelength λ. Note that the intensity profile is multiplied by $\sin(\phi)$, which is independent of θ, so that the details of the birefringence and incident wavelength of light do not modify the θ dependence of the intensity profile.[6] Now we are prepared to discuss the detection of the probability distribution of (5). Figure 5(a) shows the probability distribution as a function of angle as calculated from (5) for both cases: QED interaction between two birefringent materials, $U(\theta) \cong \frac{1}{2} A \cos(2\theta)$, and no angular QED interaction, $U(\theta) = 0$. As expected, the anisotropic disk has a higher probability of being found with an orientation $\theta = 0$ or π and a lower probability of being found at $\theta = \pi/2$. Figure 5(b) shows the transmitted intensity as a function of θ. Comparing figures 5(a) and (b), it is clear that lower intensities (occurring at $\theta = 0$ and π) should be detected more frequently than larger intensities (occurring $\theta = \pi/2$). Figure 5(c) shows the probability distribution as a function of intensity by combining (5) and (9), and shows the signal that would be detected in an experiment via a histogram of the intensities. By performing the experiment with both an isotropic plate and an anisotropic plate, both of the probability distributions shown in figure 5(c) should be obtainable.

4.3. Implementation

This experiment is currently being pursued in our laboratory at Harvard University. For an initial trial, we used 10 μm diameter polystyrene spheres (Duke Scientific) prepared in a tris (hydroxymethyl) aminomethane buffer solution with SDS added to obtain a double layer repulsion. The thermal fluctuations of the spheres were then recorded via a CCD camera attached to an upright microscope as shown in figure 4. The particles' centres were determined and tracked by the method of [30] with a standard deviation of less than 1/10 pixel. Figure 6 shows both

[6] Because ϕ simply scales the intensity function, our discussion in not limited to a single wavelength and can be generalized for white light. We also note that the incident intensity should be kept low in order to avoid any measurable transfer of angular momentum from the photons used for illumination.

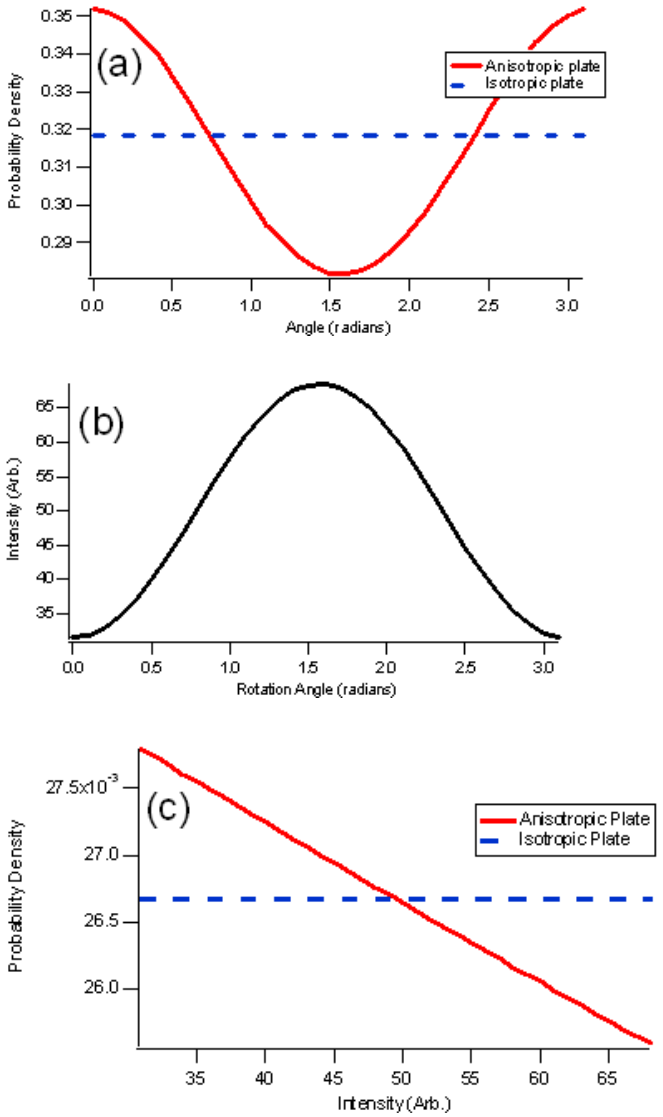

Figure 5. Probability distributions. (a) Probability of detecting a rotation θ. (b) Intensity transmitted through the experimental set-up as a function of θ. (c) Probability as a function of recorded intensity.

the tracking and intensity fluctuations recorded for one particle. Because the particle is non-birefringent, intensity fluctuations are due to scattering from imperfections in the sphere as a particle undergoes Brownian motion.

In order to study this QED torque, we want to use disks rather than spheres. Such disks are currently being fabricated using a combination of mechanical polishing and focused ion beam (FIB) sculpting for both birefringent and isotropic materials. Figure 7 shows a $LiNbO_3$ disk fabricated by crystal ion slicing [33] to produce thin $LiNbO_3$ sheets followed by FIB carving to form circular disks. Disks similar to the one shown in figure 7 are too large to undergo Brownian rotation in reasonable time frames, so smaller disks are currently being fabricated. Experiments with these disks are expected in the coming months.

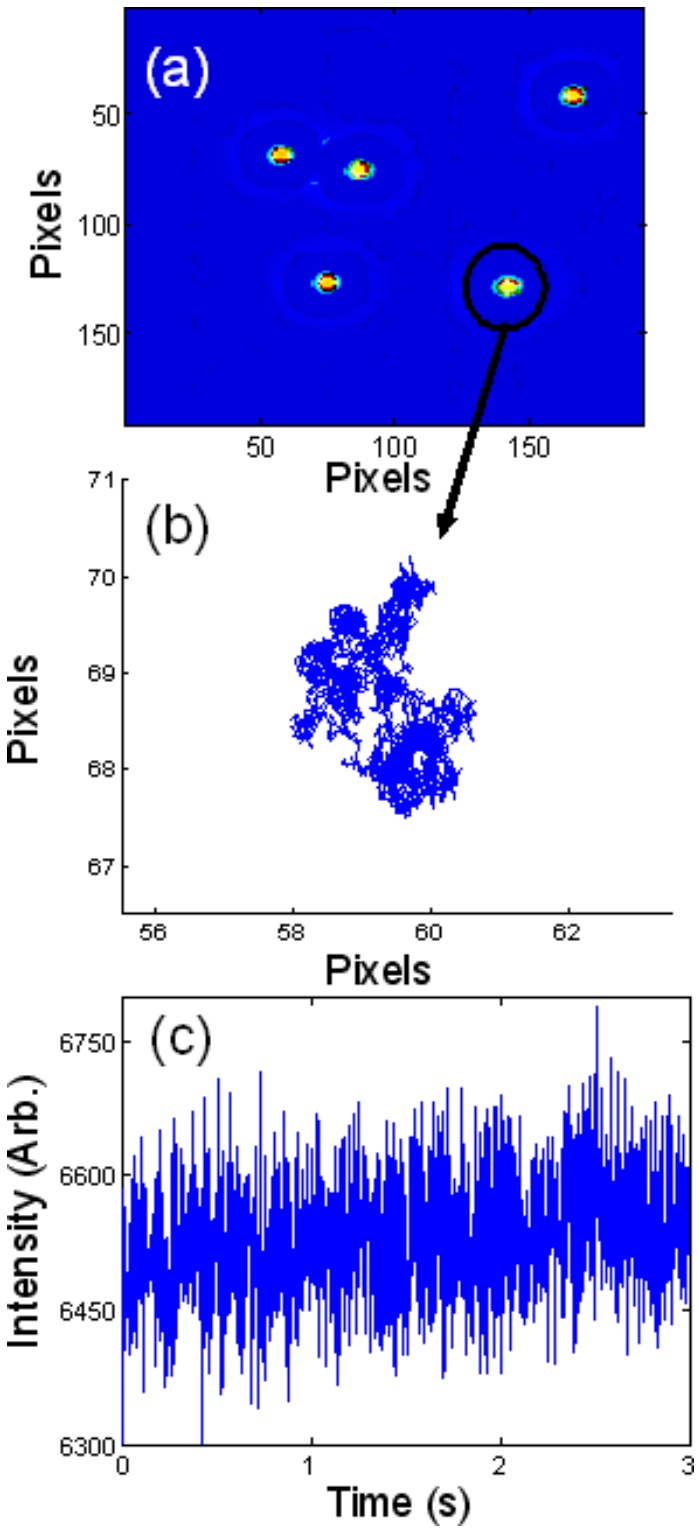

Figure 6. Computerized tracking and intensity fluctuations for 10 μm polystyrene spheres from early calibration procedures. (a) CCD image and determination of particle centres. (b) Tracking of one sphere over 5 s. (c) Intensity fluctuations of scattered light.

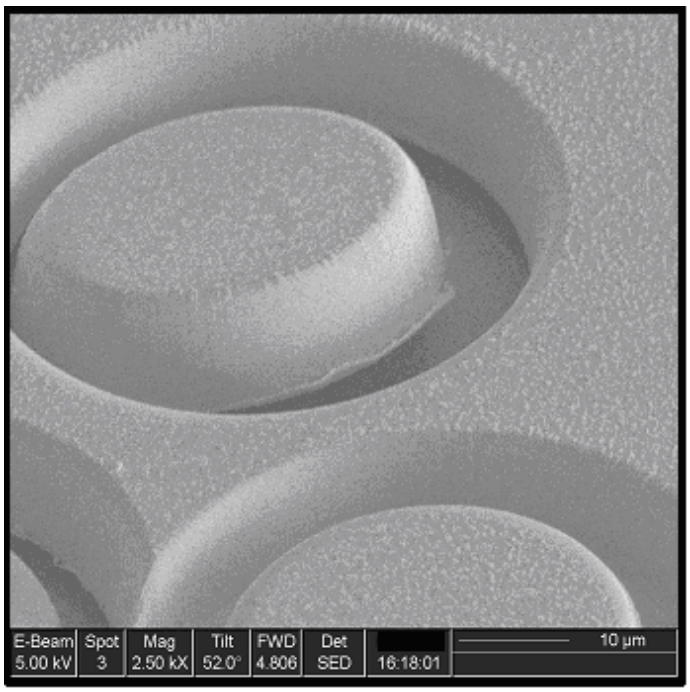

Figure 7. $LiNbO_3$ disks fabricated by crystal ion slicing and FIB sculpting.

5. Conclusions

We have considered the influence of quantum fluctuations of the electromagnetic field on a birefringent disk suspended above a birefringent plate immersed in a fluid and have proposed an experiment capable of detecting this influence. For large plates, a macroscopic QED torque should result causing two of the principal axes of the materials to align; however, as the size of the disk is reduced, Brownian motion becomes important and can disrupt observation of this phenomenon. By performing a statistical analysis of the orientation behaviour of a small disk under the influence of Brownian rotation, we can map out the potential energy profile of the disk as a function of angle to show the angular dependence of the energy associated with the quantum fluctuations of the electromagnetic field. Experiments are currently underway in our laboratory to explore such effects.

Acknowledgments

We thank M B Romanowsky and R Guerra for helpful suggestions and discussions and R M Osgood and R Roth for $LiNbO_3$ samples. This project was partially supported by NSEC (Nanoscale Science and Engineering Center), under NSF contract number PHY-0117795 and by the Center for Nanoscale Systems at Harvard University. JNM gratefully acknowledges financial support from the NSF Graduate Research Fellowship Program (GRFP) and DI acknowledges financial support from the Netherlands Organization for Scientific Research (NWO) through the Innovational Research Incentives Scheme Vernieuwingsimpuls VIDI-680-47-209.

References

[1] Casimir H B G 1948 *Proc. K. Ned. Akad. Wet.* **51** 793
[2] Lifshitz E M 1956 *Sov. Phys. JETP* **2** 73
[3] Mahanty J and Ninham B W 1976 *Dispersion Forces* (London: Academic)
[4] Israelachvili J N 1991 *Intermolecular and Surface Forces* (London: Academic)
[5] Sparnaay M J 1958 *Physica* **24** 751
[6] van Blokland P H G M and Overbeek J T G 1978 *J. Chem. Soc. Faraday Trans.* I **74** 2637
[7] Lamoreaux S K 1997 *Phys. Rev. Lett.* **78** 5
[8] Mohideen U and Roy A 1998 *Phys. Rev. Lett.* **81** 4549
[9] Chan H B, Aksyuk V A, Kleinman R N, Bishop D J and Capasso F 2001 *Science* **291** 1941
[10] Bressi G, Carugno G, Onofrio R and Ruoso G 2002 *Phys. Rev. Lett.* **88** 041804
[11] Decca R S, Lopez D, Fischbach E and Krause D E 2003 *Phys. Rev. Lett.* **91** 050402
[12] Lisanti M, Iannuzzi D and Capasso F 2005 *Proc. Natl Acad. Sci. USA* **102** 11989
[13] Ederth T 2000 *Phys. Rev.* A **62** 062104
[14] Lamoreaux S K 1999 *Phys. Rev.* A **59** 3149
[15] Svetovoy V B 2004 *Proc. 6th Workshop on Quantum Field Theory Under the Influence of External Conditions* (Princeton, NJ: Rinton) p 76
[16] Neto P A M, Lambrecht A and Reynaud S 2005 *Europhys. Lett.* **69** 924
[17] Chen F, Klimchitskaya G L, Mohideen U and Mostepanenko V M 2004 *Phys. Rev.* A **69** 022117
[18] Parsegian V A and Weiss G H 1972 *J. Adhes.* **3** 259
[19] Barash Y 1978 *Izv. Vyssh. Uchebn. Zaved. Radiofiz.* **12** 1637
[20] Munday J N, Iannuzzi D, Barash Y and Capasso F 2005 *Phys. Rev.* A **71** 042102
[21] van Enk S J 1995 *Phys. Rev.* A **52** 2569
[22] Kenneth O and Nussinov S 2001 *Phys. Rev.* D **63** 121701
[23] Shao C G, Tong A H and Luo J 2005 *Phys. Rev.* A **72** 022102
[24] Torres-Guzmán J C and Mochán W L 2006 *J. Phys. A: Math. Gen.* **39** 6791
[25] Milling A, Mulvaney P and Larson I 1996 *J. Colloid Interface Sci.* **180** 460
Meurk A, Luckham P F and Bergstrom L 1997 *Langmuir* **13** 3896
Lee S and Sigmund W M 2001 *J. Colloid Interface Sci.* **243** 365
[26] Tanzosh J P and Stone H A 1996 *Chem. Eng. Commun.* **333** 148
[27] Prieve D C and Frej N A 1990 *Langmuir* **6** 396
[28] Prieve D C 1999 *Adv. Colloid Interface Sci.* **82** 93
[29] Russel, Saville and Schowalter 1989 *Colloidal Dispersions* (Cambridge: Cambridge University Press)
[30] Crocker J C and Grier D G 1996 *J. Colloid Interface Sci.* **179** 298
[31] Jones R C 1941 *J. Opt. A.* **31** 488
[32] Fowles G R 1968 *Introduction to Modern Optics* (New York: Dover)
[33] Levy M, Osgood R M, Liu R, Cross L E, Cargill III G S, Kumar A and Bakhru H 1998 *Appl. Phys. Lett.* **73** 2293